Diagn Interv Radiol 2013; 19:393-399

MUSCULOSKELETAL IMAGING
PICTORIAL ESSAY

MRI of bone marrow abnormalities in hematological malignancies

Jose Roberto Silva Jr., Daichi Hayashi, Takenori Yonenaga, Kunihiko Fukuda, Harry K. Genant, Chieh Lin, Alain Rahmouni, Ali Guermazi

ABSTRACT
Magnetic resonance imaging (MRI) is essential for evaluating bone marrow. Bone marrow undergoes constant modification and its appearance on MRI changes in response. Knowledge of the types of changes and their origins is essential for analysis of MRI findings of bone marrow infiltration with hematological malignancies. This pictorial review describes the MRI pulse sequences used for imaging of bone marrow, and illustrates bone marrow changes due hematological malignancies, including changes following treatment.

From the Department of Radiology (J.R.S. Jr., D.H., A.G. ✉ guermazi@bu.edu), Boston University School of Medicine, Boston, Massachusetts, USA; the Department of Radiology (D.H., T.Y., K.F.), Jikei University School of Medicine, Tokyo, Japan; the Department of Radiology (H.K.G.), University of California at San Francisco, San Francisco, California, USA; Universite de Paris XII (C.L., A.R.), Creteil, France; the Department of Nuclear Medicine and Molecular Imaging Center (C.L.), Chang Gung Memorial Hospital, Gueishan, Taiwan.

Received 19 February 2013; revision requested 20 March 2013; revision received 20 March 2013; accepted 28 March 2013.

Published online 3 June 2013.
DOI 10.5152/dir.2013.067

Magnetic resonance imaging (MRI) is the only imaging method that enables direct visualization of the bone marrow with high anatomical resolution and excellent soft tissue contrast. The MRI appearance of bone marrow depends on the amounts and proportions of yellow and red marrow, which change with age and environmental factors. Red marrow contains about 40% fat, 40% water, and 20% proteins, and a proportion of 60% hematopoietic cells to 40% fat cells (1). Yellow marrow has a sparse vascular supply, and contains mainly fat (80%) and a small proportion of water (15%), with 95% fat cells. Conversion from red to yellow marrow is generally completed by 25–30 years of age. In adults, red marrow represents only half the marrow content and it is located predominantly in the axial skeleton and proximal limbs (2).

MRI sequences used for bone marrow imaging

T1-weighted imaging

T1-weighted spin-echo sequences are the most useful for evaluating bone marrow. Lipid protons have short T1 relaxation times, so the fatty marrow appears hyperintense on T1-weighted images, similar to subcutaneous fat. Red marrow has an intermediate T1 relaxation time, with a lower signal than subcutaneous fat, but a higher one than intervertebral disc or muscle (1).

T2-weighted imaging with fat suppression

T2-weighted fast spin-echo sequences can also be used to evaluate bone marrow and are the sequences used most commonly in a clinical setting. Fat suppression is required to differentiate red and yellow marrow. On fat-suppressed T2-weighted fast spin-echo sequences, the signal intensity of red marrow is higher than that of yellow marrow (1), giving better bone marrow contrast than non-fat-suppressed sequences.

Short tau inversion recovery (STIR) sequence

This technique is used to cancel the fat signal of the marrow with a 180° inversion pulse and yields high tissue contrast. The STIR sequence generally produces more homogeneous fat suppression than T2-weighted fast spin-echo sequences, but the main drawback of this sequence is that it cancels every signal close to that of fat.

Gadolinium-enhanced T1-weighted imaging

Gadolinium-enhanced T1-weighted images might be helpful for detecting some marrow lesions. Gadolinium enhancement of the normal bone marrow in adults is generally imperceptible on T1-weighted spin-

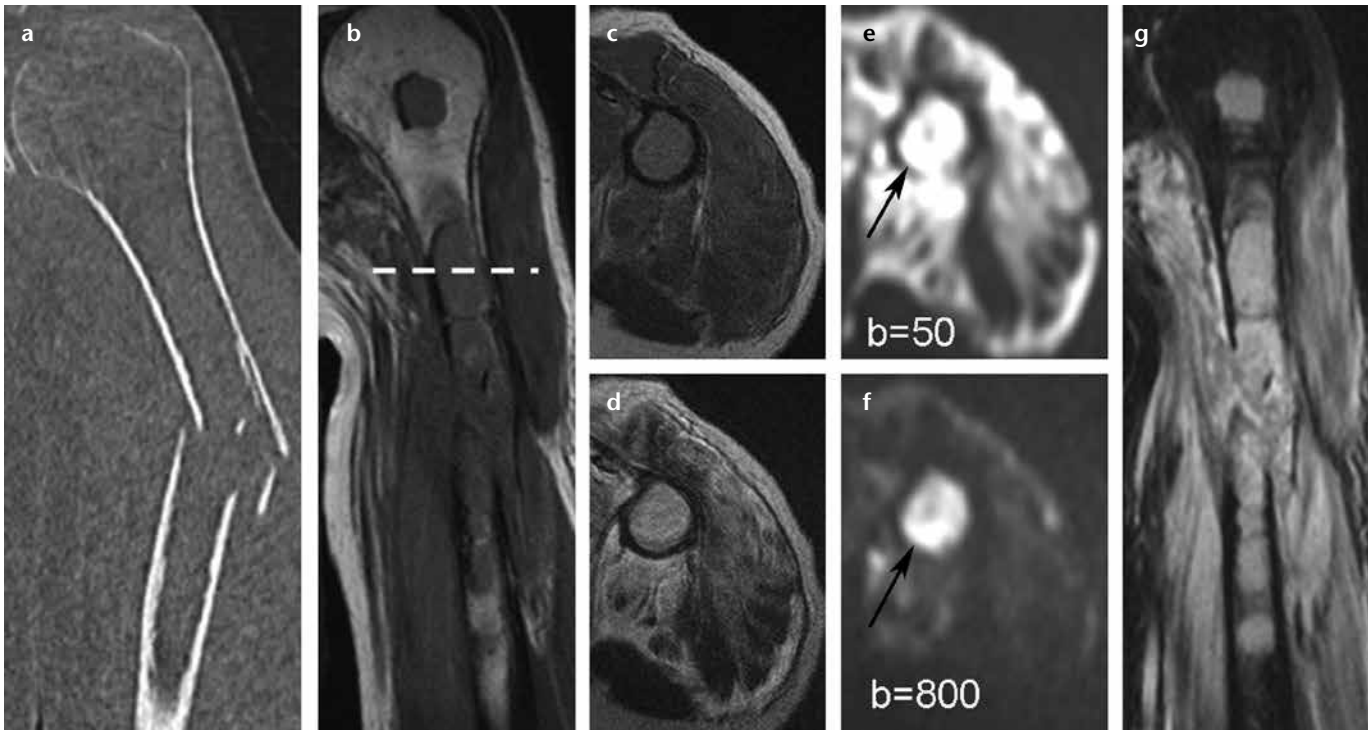

Figure 1. a–g. A 79-year-old male presented with left arm pain following a fall. Radiographs (not shown) and coronal-reformatted CT image **(a)** shows a humeral shaft fracture. A pathological fracture was suspected. The coronal T1-weighted image **(b)** shows abnormal hypointensity in the humeral bone marrow, extending to the humeral head. Axial T1-weighted **(c)** and T2-weighted **(d)** images at the level of the dotted line in **(b)** show hypointensity and intermediate signal intensity, respectively, of the humeral bone marrow. The extensive intramuscular and perimuscular hematoma resulting from the injury is seen as hyperintensity in both **(c)** and **(d)**. On both low b **(e)** and high b **(f)** diffusion weighted images, the humeral bone marrow is hyperintense *(arrows)*, with low ADC values (not shown). The lesion is hyperintense in the coronal STIR image **(g)**, suggesting the loss of normal fatty marrow. A biopsy of the lesion at the fracture site yielded a diagnosis of multiple myeloma.

echo sequences and tends to decrease significantly with increasing age and conversion to yellow marrow (3).

Dynamic contrast-enhanced MRI

Strong enhancement in both routine and dynamic contrast studies is a normal finding in many pathological processes and is a nonspecific finding. Contrast-enhanced sequences have been used in patients with lymphoproliferative diseases to demonstrate diffuse marrow infiltration, as well as to evaluate the response to chemotherapy (4). However, dynamic imaging techniques have not yet found routine clinical application.

Diffusion-weighted imaging

A malignant mass will exhibit hyperintensity in both low (e.g., b=50) and high b values (e.g., b=800) diffusion-weighted images and have low apparent diffusion coefficient (ADC) values. The most important clinical application of diffusion-weighted imaging of bone marrow is differentiating a benign fracture and the surrounding reactive edema from a pathological fracture at the site of malignant infiltration (Fig. 1) (5).

Chemical-shift imaging

On in-phase images, normal yellow and red marrow both appear hyperintense. On out-phase images, red marrow appears hypointense, while yellow marrow appears hyperintense (6). Some non-neoplastic causes can mimic the findings of malignancy on out-of-phase MRI and require a biopsy for confirmation.

Proton MRI spectroscopy

This technique can quantify the reduction in fat in infiltrative lesions and the increase in fat content with age. However, the clinical use of this sequence has not been reported, likely because the same information can be obtained using other MRI sequences.

MRI of bone marrow infiltration in hematological malignancies

The thoracolumbar spine and pelvic girdle are the main sites of hematological malignancies. MRI findings are usually nonspecific, showing hypointensity on T1- and hyperintensity on T2-weighted images. This pattern of marrow involvement can also be found in non-neoplastic marrow disorders, such as inflammatory or metabolic diseases. In addition, profound red marrow reconversion might be difficult to differentiate from malignancy. The low specificity is the main limitation of this method, but MRI still plays an important role in the initial diagnosis of hematological malignancies and might help to determine the extent of the disease, guide a biopsy, assess the response to treatment, and provide a prognosis.

Lymphoma

The malignant lymphomas, Hodgkin's and non-Hodgkin's lymphoma, represent 3%–5% of all malignancies worldwide. By definition, bone marrow involvement found in 5%–15% of patients with Hodgkin's lymphoma and in 20%–40% of non-Hodgkin's lymphoma patients (7) indicates stage IV disease. This has both therapeutic

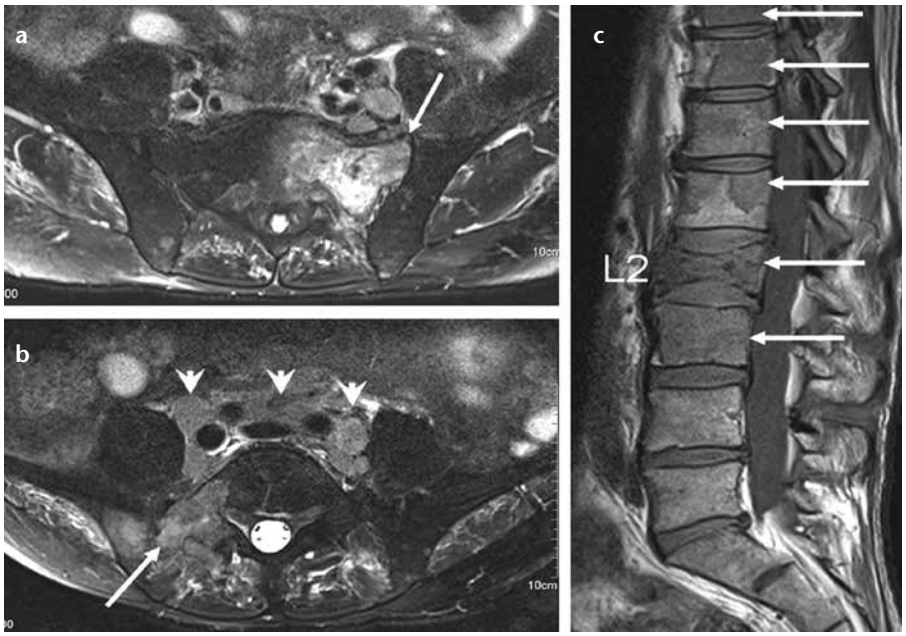

Figure 2. a–c. A 57-year-old male who was diagnosed with diffuse large B-cell lymphoma with bone marrow infiltration following a biopsy. The axial fat-saturated T2-weighted image **(a)** shows a fracture in the left sacrum (*arrow*) and surrounding diffuse hyperintensity. The hyperintensity on the MRI alone can indicate reactive edema or malignant bone marrow infiltration. In this patient, it was thought to be a pathological fracture at the site of lymphomatous infiltration because of the absence of a history of trauma and the known widespread bone marrow infiltration. Additional diffusion-weighted MRI would have helped to distinguish between benign and malignant fractures: hyperintensity in both low b and high b value images with low ADC values would have confirmed malignant infiltration, as shown in Fig. 1. The axial fat-saturated T2-weighted image at a different level **(b)** shows a malignant mass *(arrow)*. Also note the perivascular lymph node enlargement *(arrowheads)*. The sagittal T1-weighted image **(c)** shows abnormal hypointensity in the T9–11 and L1–3 vertebrae *(arrows)* and a compression fracture of the L2 body. This fracture was also considered to be a pathological fracture.

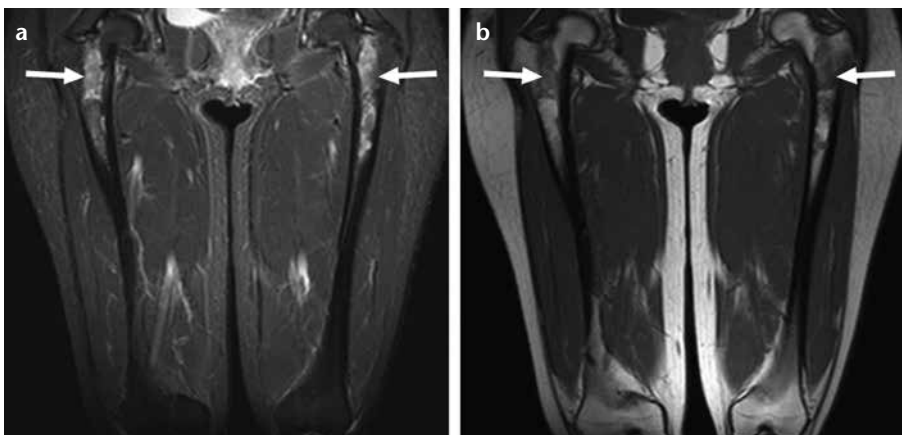

Figure 3. a, b. Acute myelogenous leukemia in a 34-year-old female presenting with a recurrence of pancytopenia six months after a bone marrow transplant to treat myelodysplastic syndrome. The coronal STIR image **(a)** shows heterogeneous hyperintensity at the proximal femur *(arrows)*, extending from the femoral neck to the subtrochanteric zone. These changes are consistent with an increase in red marrow in the proximal femur. Normal fatty marrow is seen as hypointense. The coronal T1-weighted spin-echo image **(b)** shows that the corresponding areas are hypointense *(arrows)*. Normal fatty marrow is isointense to the subcutaneous fat. A bone marrow biopsy confirmed secondary acute myelogenous leukemia (M0).

and prognostic implications. In patients with malignant lymphoma (Fig. 2), MRI is a sensitive method for detecting bone marrow involvement, which can be diffuse, focal, or located outside the iliac crest.

Lymphomatous lesions typically have longer T1 and T2 relaxation times than normal yellow and red marrow, demonstrating low signal intensity on T1-weighted and high signal intensity on fat-saturated T2-weighted or STIR sequences. Whole-body MRI has been used in patients with lymphoma to detect bone marrow metastases throughout the skeleton, particularly in children (8), and for complete staging of the lymphoma (9). MRI is also useful

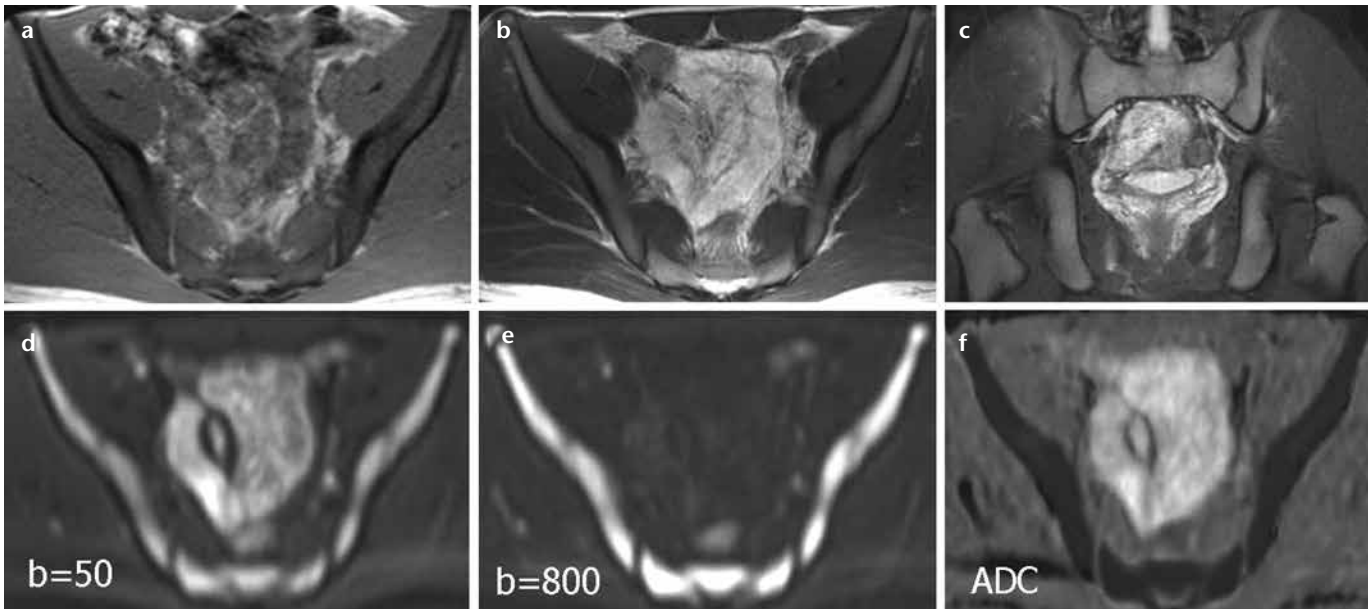

Figure 4. a–f. Acute lymphocytic leukemia in a 21-year-old male presenting with fever and hip pain. Pelvic MRI shows signal abnormalities within the iliac bone, sacrum, and proximal femurs. The axial T1-weighted image **(a)** shows diffusely hypointense bone marrow. The axial T2-weighted image **(b)** shows intermediate intensity. The axial STIR image **(c)** shows no signal suppression. Axial diffusion-weighted images **(d, e)** show marked hyperintensity. Axial ADC **(f)** shows low values.

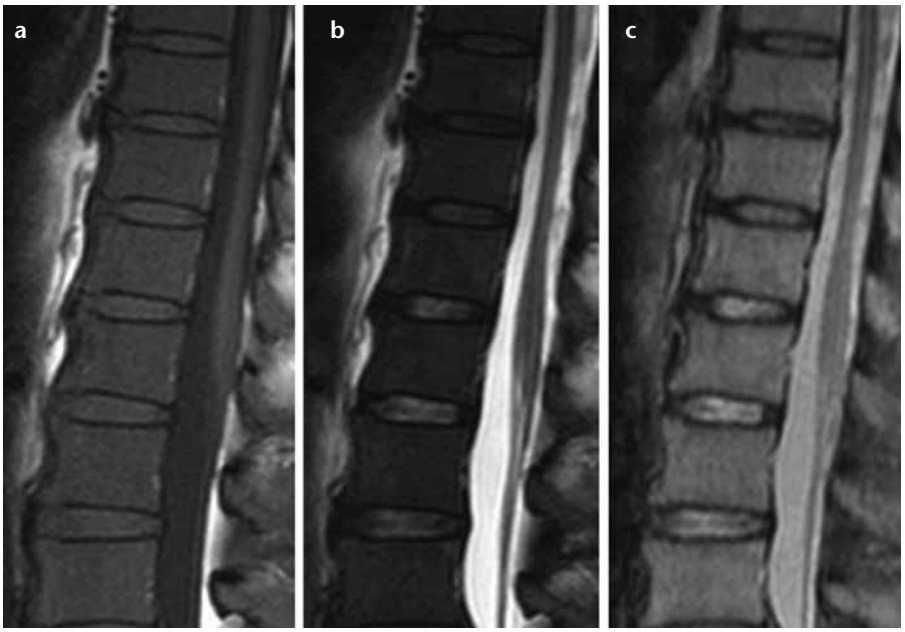

Figure 5. a–c. Myelodysplastic syndrome in a 69-year-old female with pancytopenia. The bone marrow aspiration was a dry tap. The sagittal T1-weighted image **(a)** shows bone marrow with low to intermediate signal intensity. The sagittal T2-weighted image **(b)** shows diffusely hypointense bone marrow, and the sagittal STIR image **(c)** shows no signal suppression. These findings are consistent with myelodysplastic syndrome. The bone marrow biopsy demonstrated hypercellular marrow involving all three cell lineages. The patient later developed acute myelogenous leukemia.

for guiding a blind bone marrow biopsy (10).

Leukemia

Leukemia includes a heterogeneous group of neoplasms that infiltrate bone marrow with mature or immature cells of the white blood cell lineage. In leukemia, bone marrow infiltration usually occurs diffusely, with a diffuse decrease in the marrow signal intensity on T1-weighted images (Figs. 3 and 4). MRI is highly sensitive for detecting bone marrow infiltration, but its specificity is poor, leaving the diagnosis of leukemia to peripheral blood smears and bone marrow biopsy.

Myelodysplastic syndrome

Myelodysplastic syndrome is a chronic myeloproliferative disorder that can result from an abnormal proliferation of hematopoietic stem cells (idiopathic myelofibrosis) or be secondary to several malignant and nonmalignant diseases. Typically, MRI shows hypointensity on T1- and T2-weighted images in the late stage of fibrosis (Fig. 5) (11).

Multiple myeloma

Multiple myeloma is the neoplastic proliferation of B lymphocytes with plasma cell differentiation. Multiple myeloma constitutes about 1% of all malignant diseases and about 10% of hematological malignancies (12). On MRI, the bone marrow infiltration can show various patterns, ranging from normal to focal or diffuse, or a "salt-and-pepper" appearance. Spinal compression fractures occur in 55%–70% of patients. In general, abnormalities are identified as hypointensities on T1-weighted images and hyperintensities on STIR images. Lin et al. (13) demonstrated that whole-body dynamic contrast-enhanced MRI can be

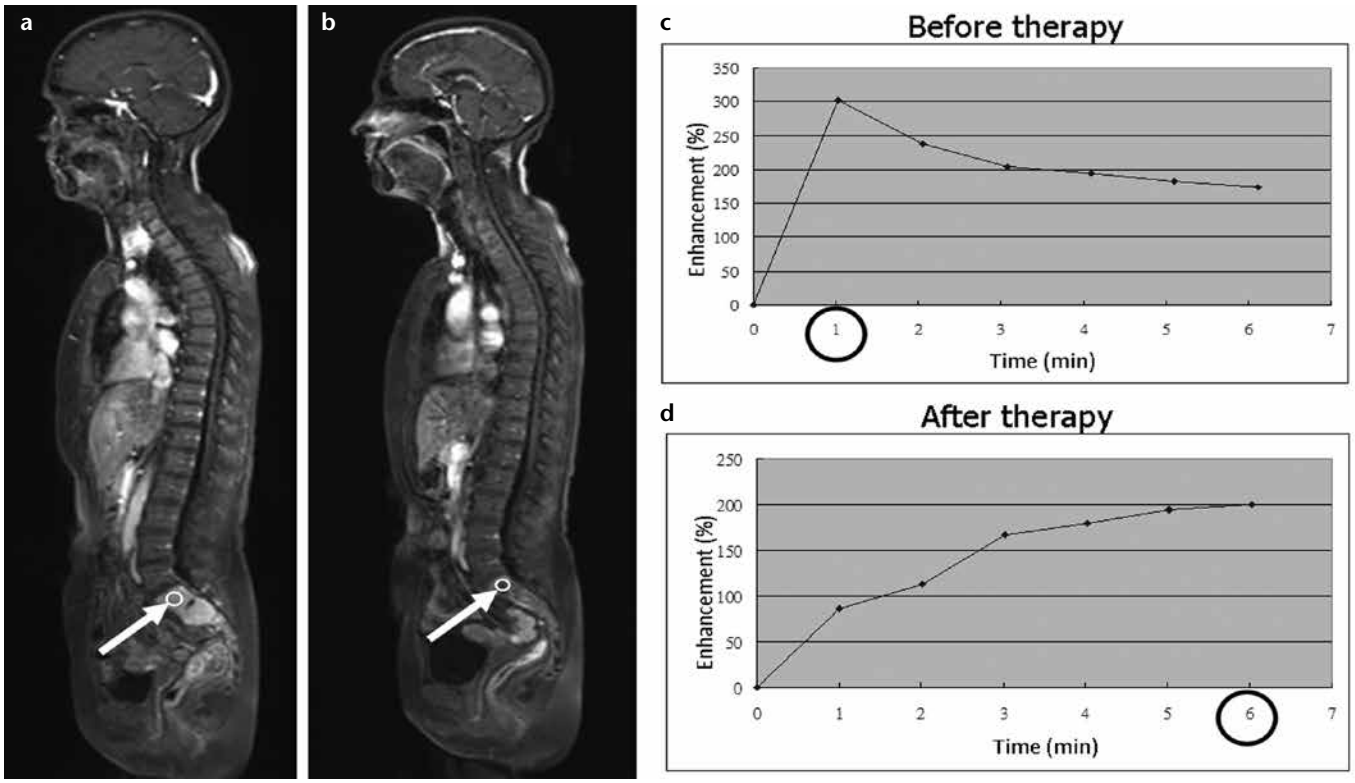

Figure 6. a–d. A 64-year-old female before and after induction chemotherapy for multiple myeloma. The sagittal fat-suppressed dynamic contrast-enhanced T1-weighted image of the spine **(a)** shows a lesion with early enhancement after contrast administration *(arrow).* The sagittal fat-suppressed dynamic contrast-enhanced T1-weighted image after therapy **(b)** shows late enhancement of the same location, indicating post-therapeutic edema *(arrow)*. The maximum focal lesion enhancement was seen at 1 min before therapy **(c)** and at 6 min after therapy **(d)**.

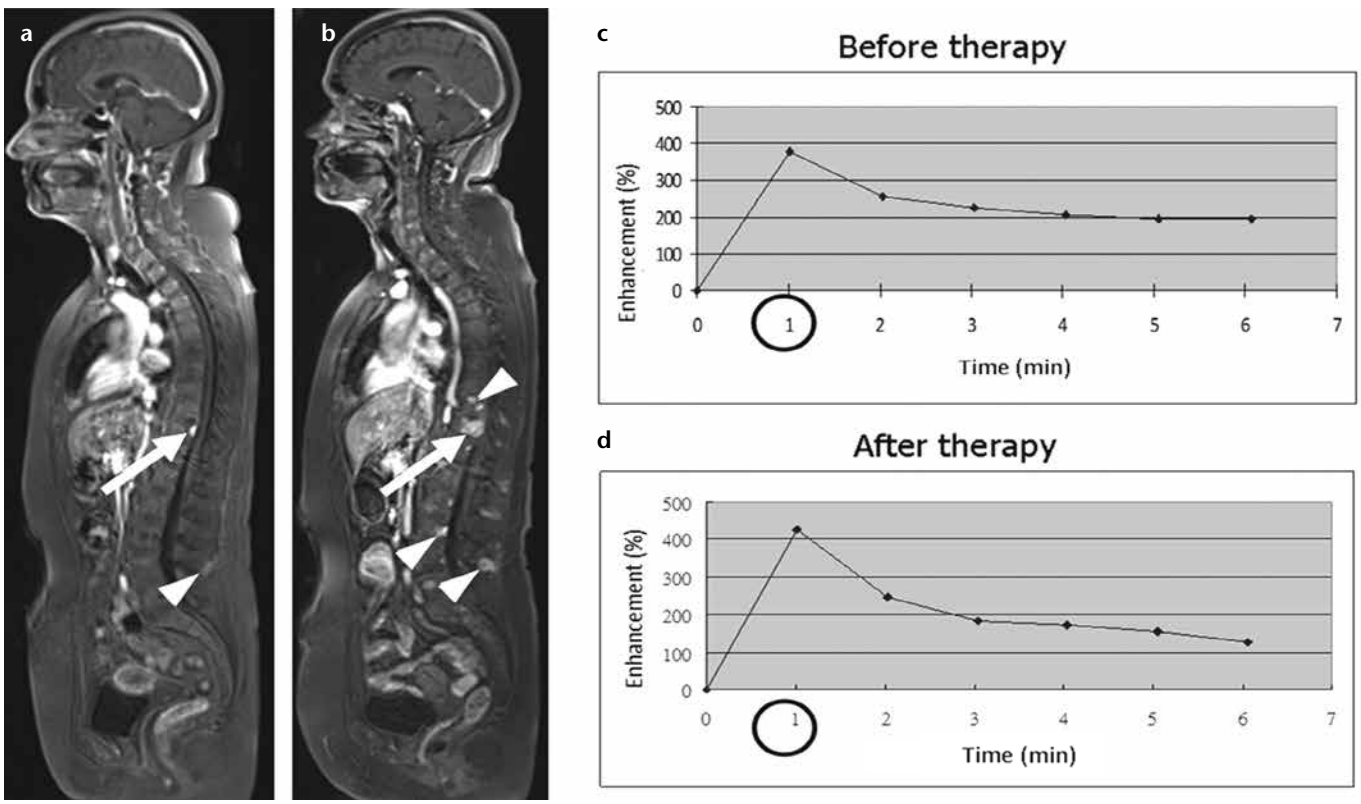

Figure 7. a–d. A 63-year-old female with multiple myeloma. Before autologous stem cell transplantation, the M-protein IgA level was 37 g/L (images not shown). Subsequent analysis showed an M-protein IgA level of 0 g/L, consistent with a complete response according to international criteria. However, the whole-body dynamic contrast-enhanced MRI **(a)** shows multiple active focal lesions demonstrating early enhancement (*arrow and arrowhead*). Two months later, progression of these focal lesions is obvious on this dynamic contrast-enhanced MRI **(b,** *arrow and arrowheads***)**. The maximum focal lesion enhancement was recorded at 1 min postinjection before **(c)** and after **(d)** therapy.

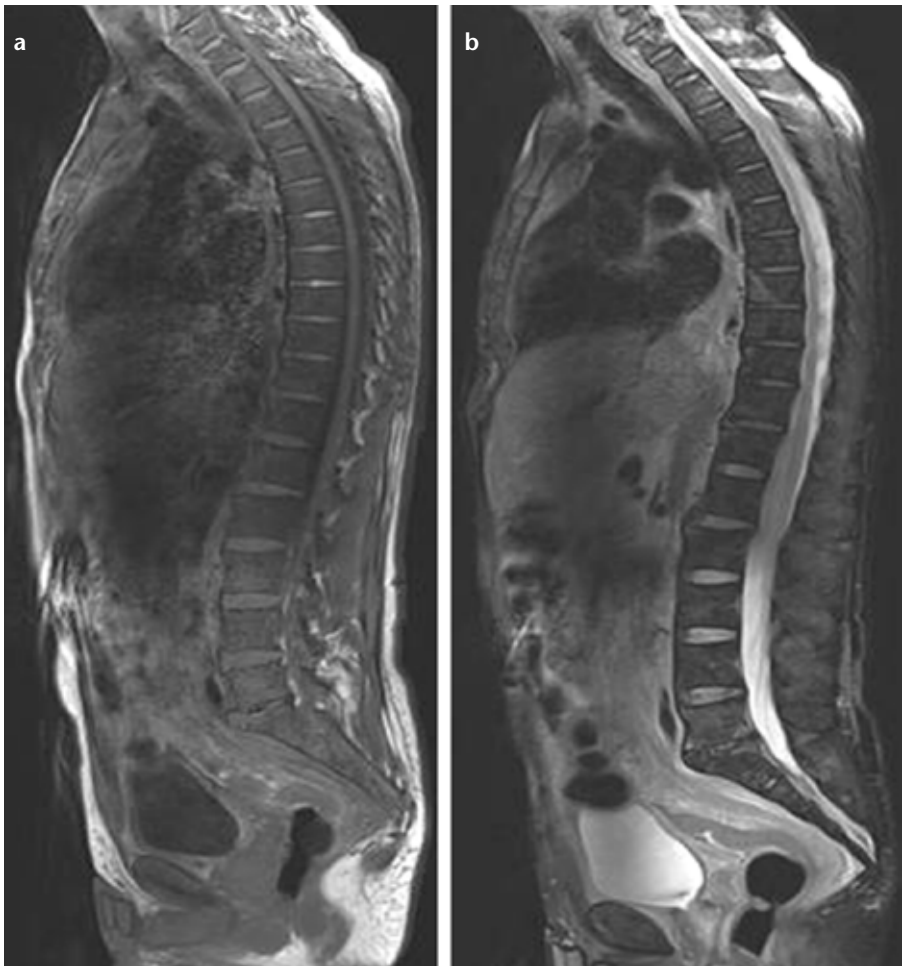

Figure 8. a, b. A 55-year-old male with Waldenström macroglobulinemia secondary to amyloidosis. The sagittal T1-weighted image **(a)** shows that bone marrow in the vertebral bodies and the sacrum is diffusely hypointense. The sagittal T2-weighted fat-saturated image **(b)** shows slight hyperintensity. Also note the extensive accumulation of amyloid in the peritoneum and retroperitoneum.

used to assess the treatment response in patients with multiple myeloma (Figs. 6 and 7).

Plasmacytoma

A bone marrow plasmacytoma is characterized by the presence of a single bone lesion or single extramedullary soft tissue mass, with an infiltrate of clonal plasma cells and absence of myeloma-type cells in the bone marrow. The most common sites in adults are the spine, pelvis, ribs, and femur. Plasmacytomas can occur in various locations. Studies have shown that the MRI findings correlate with treatment response and survival (14).

Waldenström macroglobulinemia

Waldenström macroglobulinemia is a low-grade lymphoid malignancy that usually infiltrates the bone marrow, lymph nodes, and spleen with abnormal lymphoplasmacytoid cells. It is relatively rare, accounting for 1%–2% of all hematological malignancies (15). This pathology presents with a diffuse pattern of bone marrow infiltration, as hypointensities on T1-weighted images and hyperintensities on STIR images, which are similar to multiple myeloma, but focal lesions are not identified (Fig. 8).

Post-therapeutic changes

MRI plays an important role in evaluating the response to therapy (Figs. 6, 7, and 9) and for detecting benign bone marrow complications during irradiation or chemotherapy. Treatment usually causes local or generalized changes in the bone marrow signal intensity on MRI. Initially, the bone marrow develops edema, which appears hypointense on T1-weighted images and hyperintense on fat-saturated T2-weighted and STIR images. Ultimately, the bone marrow undergoes conversion to fat, which appears hyperintense on T1-weighted and hypointense on fat-saturated images (16). The extent of the MRI signal changes in the bone marrow during and after irradiation is time- and dose-dependent (12).

Conclusion

MRI plays an important role in the diagnosis, staging, and post-treatment follow-up of hematological malignancies. Due to the low specificity of MRI, the findings need to be correlated with the clinical examination, laboratory analysis, and histopathological study for a definitive diagnosis.

Conflict of interest disclosure

The authors declared no conflicts of interest.

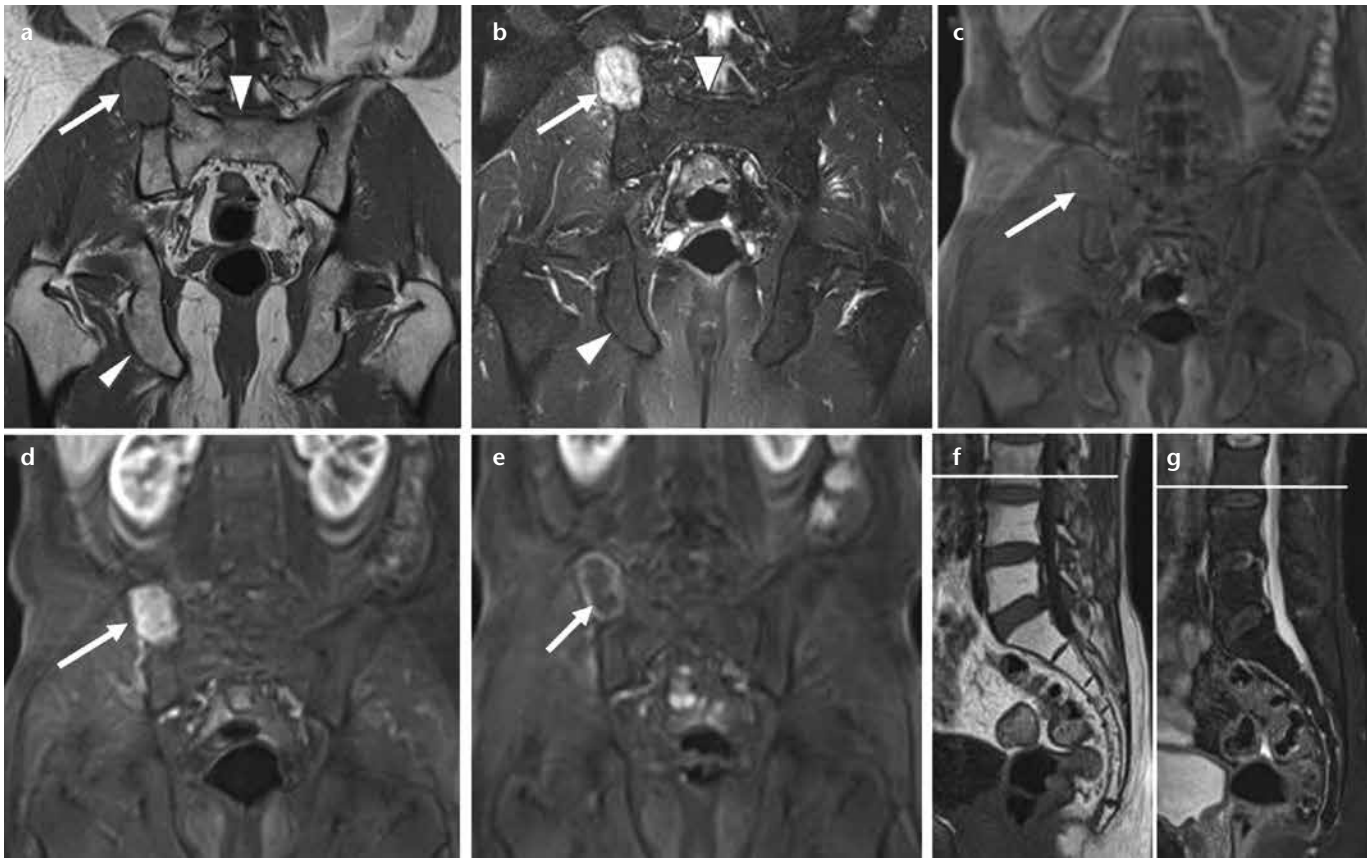

Figure 9. a–g. Fatty conversion following therapy in a 57-year-old male with multiple myeloma in the right iliac bone. Before chemotherapy and radiation therapy, the coronal T1-weighted image **(a)** depicted the lesion as a hypointense oval mass *(arrow),* and the coronal T2-weighted fat-saturated image **(b)** showed a hyperintense mass *(arrow)*. Note the normal signal intensity of the sacral and pelvic bones, both of which show heterogeneous hyperintensity on the T1-weighted image (**a,** *arrowheads*) and hypointensity (**b,** *arrowheads*) on the T2-weighted image. On the diffusion-weighted image, the lesion is hyperintense on low- and high b images, and the diffusion is restricted (not shown). The coronal T1-weighted fat-saturated images before **(c)** and after **(d)** contrast administration show strong enhancement of the lesion *(arrows)*. After chemotherapy and radiotherapy, the coronal T1-weighted fat-saturated image **(e)** of the myeloma lesion does not show enhancement on the contrast-enhanced image *(arrow)* and is no longer hypercellular; i.e., it is hyperintense on low b and hypointense on high b, with nonrestricted diffusion (not shown). The sagittal T1-weighted image **(f)** shows the bone marrow of the L4 and L5 vertebrae, as well as the sacroiliac bones with homogeneous hyperintensity, and the sagittal fat-saturated T2-weighted image **(g)** shows homogeneous hypointensity. These findings represent post-therapeutic fatty conversion of the bone marrow.

References

1. Vande Berg BC, Malghem J, Lecouvet FE, Maldague B. Magnetic resonance imaging of normal bone marrow. Eur Radiol 1998; 8:1327–1334. [CrossRef]
2. Blebea JS, Houseni M, Torigian DA, et al. Structural and functional imaging of normal bone marrow and evaluation of its age-related changes. Semin Nucl Med 2007; 37:185-194.
3. Montazel JL, Divine M, Lepage E, Kobeiter H, Breil S, Rahmouni A. Normal spinal bone marrow in adults: dynamic gadolinium-enhanced MR imaging. Radiology 2003; 229:703–709. [CrossRef]
4. Rahmouni A, Montazel JL, Divine M, et al. Bone marrow with diffuse tumor infiltration in patients lymphoproliferative diseases: dynamic gadolinium-enhanced MR imaging. Radiology 2003; 229:710–717. [CrossRef]
5. Karchevsky M, Babb JS, Schweitzer ME. Can diffusion-weighted imaging be used to differentiate benign from pathologic fractures? A meta-analysis. Skeletal Radiol 2008; 37:792–795. [CrossRef]
6. Disler DG, McCauley TR, Ratner LM, Kesack CD, Cooper JA. In-phase and out-of-phase MR imaging of bone marrow: prediction of neoplasia based on the detection of coexistent fat and water. AJR Am J Roentgenol 1997; 169:1439–1447. [CrossRef]
7. Wang J, Weiss LM, Chang KL, et al. Diagnostic utility of bilateral bone marrow examination: significance of morphologic and ancillary technique study in malignancy. Cancer 2002; 94:1522–1531. [CrossRef]
8. Parker GJ, Suckling J, Tanner SF, Padhani AR, Husband JE, Leach MO. MRIW: parametric analysis software for contrast-enhanced dynamic MR imaging in cancer. Radiographics 1998; 18:497–506.
9. Kellenberg CJ, Epelman M, Miller SF, Babyn PS. Fast STIR whole-body MR imaging in children. Radiographics 2004; 24:1317–1330. [CrossRef]
10. Kwee TC, Kwee RM, Verdonck LF, Bierings MB, Nievelstein RA. Magnetic resonance imaging for the detection of bone marrow involvement in malignant lymphoma. Br J Haematol 2008; 141:60–68. [CrossRef]
11. Guermazi A, de Kerviler E, Cazals-Hatem D, Zagdanski AM, Frija J. Imaging findings in patients with myelofibrosis. Eur Radiol 1999; 9:1366–1375. [CrossRef]
12. Hwang S, Panicek DM. Magnetic resonance imaging of bone marrow in oncology, Part 2. Skeletal Radiol 2007; 36:1017–1027. [CrossRef]
13. Lin C, Luciani A, Belhadj K, et al. Multiple myeloma treatment response assessment with whole-body dynamic contrast-enhanced MR imaging. Radiology 2010; 254:521-531.
14. Stabler A, Baur A, Bartl R, Munker R, Lamerz R, Reiser MF. Contrast enhancement and quantitative signal analysis in MR imaging of multiple myeloma: assessment of focal and diffuse growth patterns in marrow correlated with biopsies and survival rates. AJR Am J Roentgenol 1996; 167:1029–1036. [CrossRef]
15. Herrinton LJ, Weiss NS. Incidence of Waldenstrom's macroglobulinemia. Blood 1993; 82:3148–3150.
16. Daldrup-Link HE, Henning T, Link TM. MR imaging of therapy-induced changes of bone marrow. Eur Radiol 2007; 17:743–761. [CrossRef]